Causal Autoencoder-like Generation of Feedback Fuzzy Cognitive Maps with an LLM Agent

Akash Kumar Panda
Department of Electrical and Computer Engineering
University of Southern California
Los Angeles, USA
akashpan@usc.edu

Olaoluwa Adigun
School of Computing and Information Sciences
Florida International University
Miami, USA
olaadigu@fiu.edu

Bart Kosko
Department of Electrical and Computer Engineering
University of Southern California
Los Angeles, USA
kosko@usc.edu

***Abstract*—A large language model (LLM) can map a feedback causal fuzzy cognitive map (FCM) into text and then reconstruct the FCM from the text. This explainable AI system approximates an identity map from the FCM to itself and resembles the operation of an autoencoder (AE). Both the encoder and the decoder explain their decisions in contrast to black-box AEs. Humans can read and interpret the encoded text in contrast to the hidden variables and synaptic webs in AEs. The LLM agent approximates the identity map through a sequence of system instructions that does not compare the output to the input. The reconstruction is lossy because it removes weak causal edges or rules while it preserves strong causal edges. The encoder preserves the strong causal edges even when it trades off some details about the FCM to make the text sound more natural.**

***Index Terms*—Causal reasoning, autoencoders, fuzzy cognitive map, feedback dynamics, explainable AI, agentic AI**

I. Generating Causal Feedback Fuzzy Cognitive Maps by Identity Approximations

How do we generate representative text from a causal feedback semantic network? This task is at least as difficult as the reverse problem of how do we reliably map text to a causal feedback semantic network such as a feedback fuzzy cognitive map (FCM) [1]–[8] dynamical system.

We harness large language models (LLMs) to approximate an identity map $\Phi : \mathcal{F} \to \mathcal{F}$ from the feedback causal map $F \in \mathcal{F}$ to $\Phi(F) \approx F$ by way of representative text. The mapping structure Φ resembles the forward-backward structure of autoencoders (AEs) often found in AI image generators and LLMs. But those semi-supervised maps rely on black-box neural networks with simple feedforward layers of neurons and that have no dynamics. FCM knowledge graphs are explainable AI (XAI) models that list their local causal rules in their edge matrix. Their feedback structure defines a dynamical system with rich output equilibria that can act as answers to user questions and can guide agentic-like tasks.

Figure 1 shows this autoencoder-like identity approximator. The LLM agent with the encoding prompt maps from the FCM to text. The LLM agent with the decoding prompts then maps the text back to the reconstructed FCM. The encoded text summary latent I sounds unnatural when the encoder focuses on capturing every detail of the FCM. The LLM agent with the content editing prompt can rewrite the text to make it sound more natural. But this might come with a loss in detail leading to a lossy reconstruction.

Consider an FCM that models the cause of clinical depression [9]. Column 2 of Table I gives the nodes of this FCM. The 7^{th} node C_7 represents "fatigue or loss of energy" and the 9^{th} node C_9 represents "loss of appetite". Figure 2a shows the edge matrix E of this FCM. It also shows that there is a causal edge e_{97} "loss of appetite" $\to$ "fatigue or loss of energy" with weight $w_{97} = 0.8$. The LLM agent with the encoding prompt translated this edge to this sentence in the latent I summary:

> **'Loss of appetite'** strongly causes **'fatigue or loss of energy'** and significantly increases **'psychomotor retardation'** and **'reduced interest for daily functioning'**.

The LLM agent decodes this summary as follows: C_7 is "fatigue or loss of energy", C_9 is "loss of appetite", and the edge e_{97} "loss of appetite" $\to$ "fatigue or loss of energy" has weight $w_{97} = 0.8$. The agent was too focused on capturing the exact nodes and edges so the text sounds unnatural.

The LLM agent with the content-editing prompt rewrites the text summary latent I to make it sound more natural. This gives the natural sounding text summary latent II with the corresponding sentence:

> Even a loss of **appetite** contributes to the cycle by strongly causing **fatigue** and significantly increasing **psychomotor retardation** and a loss of **interest in daily activities**.

This sentence from the latent II summary then translates to the following: C_7 is "fatigue or loss of energy", C_9 is "appetite", and the fuzzy or partial causal edge e_{97} "appetite" $\to$ "fatigue or loss of energy" has weight $w_{97} = -0.8$. Note that the source node is "appetite" instead of "loss of appetite".

1946-0759/25/$31.00 ©2025 IEEE
DOI 10.1109/ICMLA66185.2025.00188

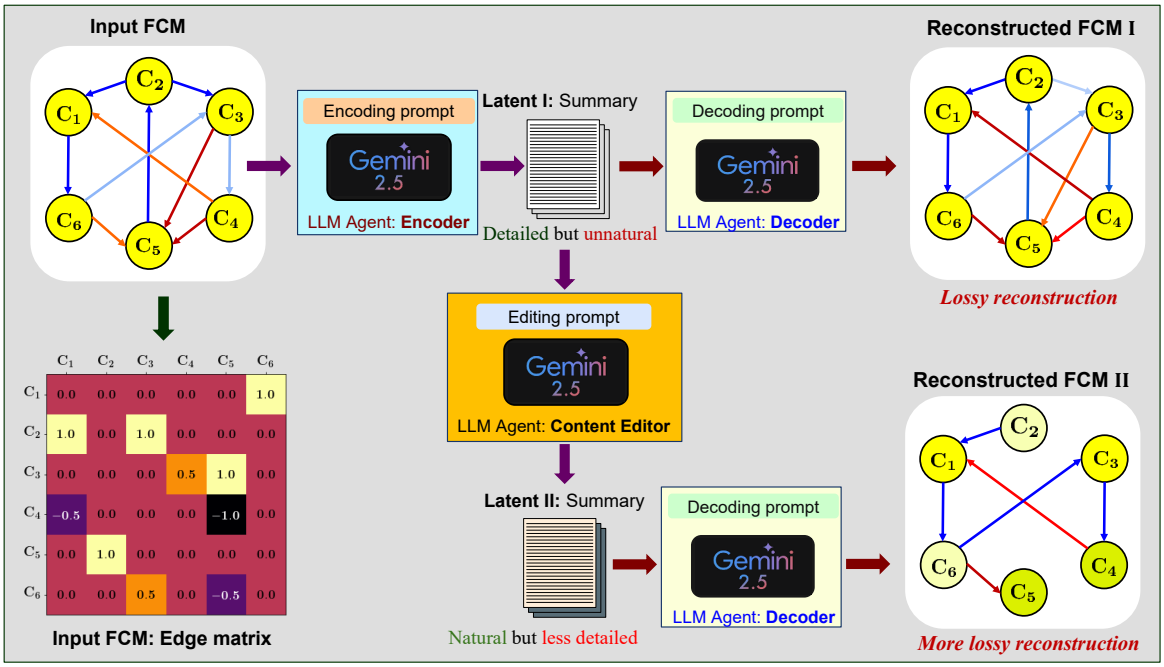

Fig. 1: Autoencoding Fuzzy Cognitive Maps (FCMs) with a single LLM agent and multi-prompting: The input FCM is on the top-left. Its edge matrix E is on the bottom-left. The edge matrix colors correspond to the edge weights. Higher edge weights correspond to brighter colors. The LLM agent with the encoding prompt converts the input FCM into the text description latent I. This text description is a detailed description of the input but sounds unnatural. The LLM agent with the content-editing prompt reworks latent I into latent II. The result sounds more natural but sacrifices some detail. The LLM agent with the decoding prompt reconstructs FCMs from their text description in latent I and latent II. The top-right FCM shows that unnatural yet detailed latent I gives a lossy FCM reconstruction. The less detailed yet natural sounding latent II gives a lossier reconstructed FCM in the bottom-right FCM.

Section II-A explains how feedback FCMs work. It shows how FCMs model causal dynamical systems as weighted directed graphs and also explains what their nodes and edges represent. This section also explains how FCMs evolve in discrete time through matrix-multiplication and nonlinear operations to give FCM limit-cycle equilibria. Section II-A concludes by showing how to mix FCMs into a new FCM. FCMs allow knowledge combination through convex mixing unlike directed acyclic graphs (DAGs) [10] or Markov chains with different states.

Section II-B discusses autoencoding and its variants including ordinary and variational autoencoder networks. This section also explains how our FCM "autoencoder" differs from the usual autoencoder networks in terms of explainability and supervision. Section II-C briefly explains LLMs and their single-agent and multi-prompting version. It shows how system instructions can manipulate the behavior of the LLM agent. This section also explains how the LLM's Natural Language Processing (NLP) and Named Entity Recognition (NER) capabilities [11] encode and reconstruct FCMs.

Section III explains how we use LLMs to map FCMs to text and then back to FCMs. It goes through every system instruction that multi-prompts LLM agent to systematically convert an FCM to text. It also goes through the system instructions that help the LLM reconstruct an FCM from its text description.

Section IV discusses our experiments and their results. Google's Gemini 2.5 Pro [12] takes 3 different FCMs as input and then converts them to their corresponding text descriptions. The Gemini LLM then reconstructs the FCMs from those text descriptions. The 1st columns of Tables I, III, and IV describe the nodes on the input FCMs. Figures 2a, 3a, and 4a show their respective edges.

The 2nd and 3rd columns of Tables I, III, and IV give the nodes of the corresponding reconstructed FCMs. Figures 2b−2d, 3b−3c, and 4b−4c show the edge matrices of those reconstructed FCMs.

Section V discusses the trade-off between natural-sounding text and FCM-reconstruction accuracy. It also shows that our lossy reconstruction still preserves the strong causal connections in the FCM. This section also explains how some nodes get flipped during FCM reconstruction.

II. How FCMs, AEs, and LLMs Work

A. Fuzzy Cognitive Maps

FCMs model causal dynamical systems as directed weighted cyclic graphs. They allow fuzzy or partial causality and feedback cycles unlike causal graphs such as Bayesian belief networks (BBNs) that allow only DAGs [10]. Feedback lets FCMs model dynamical systems with complex equilibria such as limit cycles. FCMs with *different* nodes also mix through convex combination unlike DAGs or Markov chains.

1) Causal model: The FCMs model the causal variables in the dynamical system as "concept nodes" of the directed

graph. The nodes are associated with some kind of magnitude such that the corresponding causal variable can "increase", "improve", or "intensify" because of the other causal variables of the system.

Let C_i and C_j denote the respective i^{th} and j^{th} concept nodes or causal variables in the FCM. The edge e_{ij} from C_i to C_j connects the nodes if "C_i causes C_j". The weight $w_{ij} \in [-1, 1]$ on the edge e_{ij} describes the degree to which C_i causes C_j. A positive w_{ij} means that an increase in C_i causes C_j to increase or a decrease in C_i causes C_j to decrease. A negative w_{ij} value means that an increase in C_i causes C_j to decrease or a decrease in C_i causes C_j to increase. The magnitude of w_{ij} shows the strength of the causal connection. A magnitude close to 1 denotes a "strong" causal connection and a magnitude close to 0 denotes a "weak" causal connection.

The 1st column of Table I and Figure 2a give the respective nodes C_1–C_{14} and the edge matrix E of a 14-node FCM that models causes of clinical depression [9]. The i^{th} row and the j^{th} column of the edge matrix E gives the value of w_{ij} for edge e_{ij}.

2) Discrete time-evolution: The n-dimensional row vector $C(t) \in [0, 1]^n$ represents the state of a n-node FCM at discrete time t. The k^{th} component $C_k(t)$ of this state vector $C(t)$ denotes the state of the k^{th} concept node in the FCM at time t. The k^{th} node is "active" if $C_k(t)$ is close to 1 and it is "inactive" if $C_k(t)$ is close to 0. The causal variables corresponding to the active nodes are present in the system at time t and the variables corresponding to the inactive nodes are absent from the system at time t.

The FCM's state vector $C(t)$ evolves in discrete time t through matrix-multiplication and nonlinear squashing. The state of the FCM $C(t+1)$ at time $t+1$ depends on the state of the FCM $C(t)$ at time t and on the edge matrix E:

$$C_j(t+1) = \phi\left(\sum_{i=1}^{n} C_i(t) w_{ij}\right) \tag{1}$$

where ϕ is an increasing nonlinear function bounded between zero and one.

The sequence of FCM state vectors $C(0)$, $C(1)$, $C(2)$, ... describes the trajectory of the FCM in discrete time t starting from the initial state $C(0)$. This qualitatively represents the corresponding trajectory of the dynamical system that the FCM models. The limiting behavior of this sequence gives the equilibrium behavior of the FCM. The FCM converges to a fixed point if $C(t)$ converges to a constant row-vector. The FCM converges to a k-step limit cycle if $C(t) = C(t+k)$ at some point in the trajectory. Then a sequence of k state vectors repeats itself over and over again.

The FCM equilibria partition the input space. The set of all initial states that lead to a certain equilibrium makes up the basin of that equilibrium. The map from the basins to the equilibrium characterizes the FCM and also the dynamical system that the FCM models.

3) FCM Mixing: FCMs allow mixing through convex combination. Let S_1, S_2, ..., S_m denote the respective node sets of m FCMs. The node-set of the N-node FCM mixture is $S = S_1 \cup S_2 \cup ... \cup S_m$. The $N \times N$ edge matrix $\tilde{E}_k$ pads the k^{th} FCM's edge matrix E_k with zero-rows and zero-columns corresponding to the nodes in $S - S_k$. The edge matrix E of the FCM mixture is

$$E = \sum_{k=1}^{m} v_k \tilde{E}_k \tag{2}$$

where v_k are convex mixing weights such that $v_k \geq 0$ and $\sum_{k=1}^{m} v_k = 1$.

FCM mixing is *closed*: Mixing FCMs gives back an FCM. This is not true in general for BBN DAGs or for the stochastic matrices of Markov chains. Mixed DAGs can have cycles and mixed different-state stochastic matrices may not be stochastic.

B. Autoencoders

Autoencoding is a form of identity mapping from a domain back to itself. This involves a two-step process: (1) transforming the input into a reduced form in the latent space, and (2) reconstructing the input with minimal loss. The first step is encoding and the second step is decoding. Autoencoding applies to various domains including signal processing, information theory, and statistical learning.

Autoencoder networks are a family of autoencoding models that use an encoder network and a decoder network. The encoder network maps the input data to its latent variable and the decoder network reconstructs the input data from the latent variable. Variational autoencoders are variants of autoencoder networks that map to constrained latent variables and this makes them suitable for generative tasks [13]–[16]. Autoencoder networks can solve various problems including dimensionality reduction [17], denoising [18], anomaly detection [19], image compression [20], and feature extraction [21], [22].

There are other forms of autoencoding that replace neural network models with other techniques for encoding and decoding. Examples of such techniques include Principal Component Analysis (PCA), wavelet transforms, and dictionary learning.

The encoder and the decoder networks of the autoencoder are usually black boxes and do not explain their decisions in encoding and decoding. The latent variables the encoder maps to is usually not human interpretable. Also it relies on a loss function that compares the reconstructed pattern to the input pattern.

We present a way of multi-prompting a LLM system so that it achieves an identity map from the FCM to text and back to FCM just like an autoencoder but its system instructions can explain its decisions during the encoding and the decoding process. Its latent variables are also human-interpretable text descriptions of the FCM. It can give reasons for its decisions during reconstruction by quoting from the text that the decoder takes as input. Also it achieves the identity map without having to compare the reconstructed FCM to the target FCM and

just by following a sequence of carefully designed system instructions.

C. Large Language Models (LLMs)

LLMs are AI systems that have trained on the vast corpora of human-generated text for the purpose of generating human-like language. These models use the transformer neural architecture [23] with an attention mechanism and billions or trillions of parameters to learn human linguistic patterns. This enables LLM to perform tasks such as text generation, summarization, translation, code-synthesis, and NER. LLMs have become foundational in NLP and they power chatbots, virtual assistants, and enterprise automation across industries.

Single-agent multi-prompting is a strategy where a single LLM instance uses successive multiple-structured prompts to solve a complex problem. This approach leverages the internal capabilities of the LLM agent to handle sequential or parallel subtasks using techniques such as chain-of-thought prompting, role-playing, or staged queries. Applications of single-agent multi-prompting span education, coding, planning, and decision support where task complexity is managed through prompt design rather than architectural overhead.

III. New FCM-LLM Mapping Technique

We designed a system with an LLM agent and multi-prompting to convert an input FCM to its latent summary and then reconstruct the FCM. The system used successive system instructions together with multi-prompting. The system instructions manipulate the behavior of the LLM agent. They tell the LLM agent how to process its inputs and how to structure its outputs. These instructions also specify what aspects of the input to focus on.

A. Encoding Prompt

This uses a set of system instructions that define how the LLM agent extracts the text summary latent I from the input FCM. This form of encoding maps the FCM to a detailed but unnatural summary. It takes the FCM node list and the edge-weight matrix as input

The encoding prompt also instructs the LLM to explain each edge of the input FCM as text. The LLM summarizes the causal edge weights in words. The LLM has to measure the importance of each node based on how many edges connect it to other nodes. It then has to distribute the focus of the text among the nodes based on their importance: Focus more on the nodes that are more important. The LLM also has to sound natural as it describes this.

B. Content Editing Prompt

This prompt requires a set of system instructions that define how the LLM agent rewrites the text summary latent II from the encoded text summary output latent I of the LLM agent with the encoding prompt. The LLM agent with the encoding prompt may focus more describing the FCM edges than on sounding natural. It may generate text that sounds forced and repetitive and hard to read. The LLM agent with the content editing prompt reworks the latent I summary and makes it sound more natural. This system instruction is not too specific and depends on the LLM's NLP capabilities.

C. Decoding Prompt

The decoding divides into 3 subtasks: noun detection, node detection, and edge extraction. The LLM agent uses a set of 3 successive system instructions to solve the subtasks.

1) Noun detection: This system relies on the LLM's Named Entity Recognition (NER) capabilities. It asks the LLM to take the output text from the LLM agent with the encoding or the content editing prompt and process it sentence-by-sentence. The LLM then has to detect nouns, noun phrases, and pronouns in those sentences. The LLM also matches the pronouns to their corresponding noun antecedents. The nodes in an FCM are always nouns or noun phrases that describe a causal variable in the dynamical system. The detected nouns and noun phrases serve as node candidates for the reconstructed FCM. The LLM can also explain where these node candidates come from in the text.

2) Node detection: This system uses a set of system instructions to extract nodes from nouns and noun phrases. It instructs the LLM agent to go through the list of nouns and noun phrases from node detection and then refines it into a list of FCM nodes. The FCM nodes are nouns and noun phrases that represent causal variables in the dynamical system. They have some degree of magnitude: They can either "increase", "improve", or "intensify". The LLM agent with the 'node detection' prompt goes through the list of nouns and noun phrases and looks for these properties. The LLM also checks if the text suggests a causal connection between the nouns/noun phrases. The LLM can quote from the text to give evidence of these causal connections.

3) Edge extraction: This system uses a set of instructions that describes how to extract $n^2 - n$ node-pairs from a list of n nodes. The LLM agent then goes through each node pair and looks through the text for evidence of positive, negative, or zero causal influence. The LLM then assigns the edge weights based on the language used in the text. The LLM can also quote the text to justify its choice of causal edges.

This list of edges along with the node-list completely describes the reconstructed FCM. The 2$^{\text{nd}}$ column of Table I and Figure 2b give the respective nodes and the edge matrix E_1 of an FCM reconstructed from the LLM agent's "raw" text summary latent I that described the FCM from Figure 2a and Table I's column 1.

The 3$^{\text{rd}}$ column of Table I and Figure 2c give the resepctive nodes and the edge matrix E_2 of the FCM reconstructed from the latent II text summary that describes the FCM from Figure 2a and Table I's column 1.

IV. Experiment Setup

We applied Google's Gemini 2.5 Pro LLM with "temperature = 0" and "top_p = 0.95" on three FCM inputs. The first FCM modeled the causes of clinical depression with 14 nodes and 180 edges. This densely connected FCM had only positive

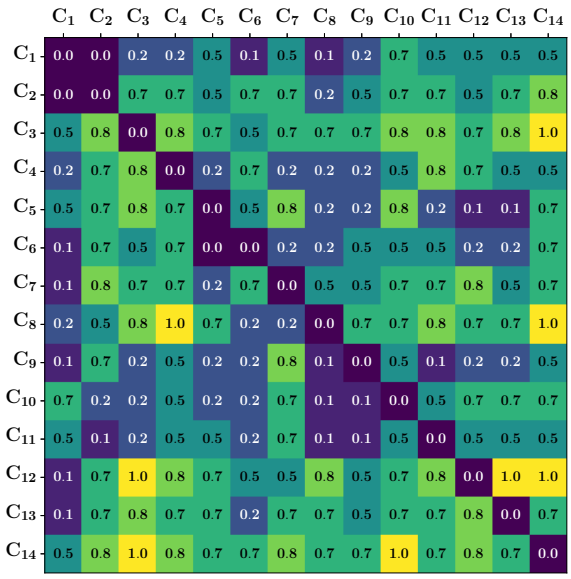

(a) Edge matrix E of the target FCM.

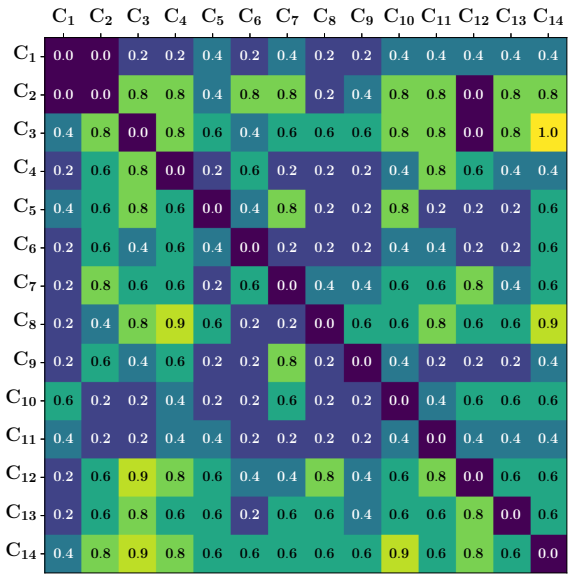

(b) Reconstructed edges E_1 from latent I.

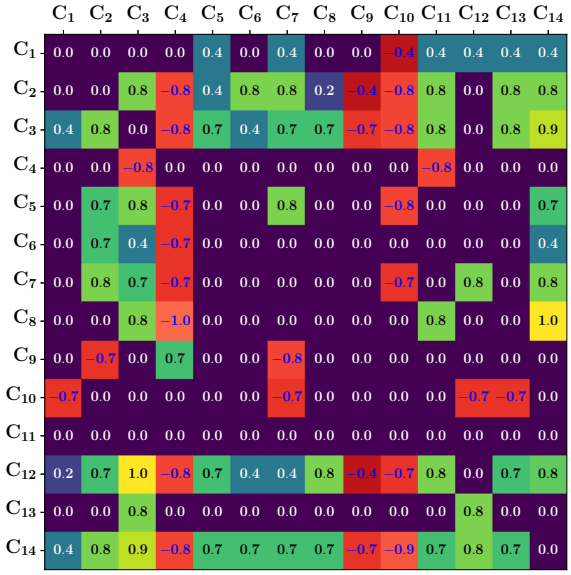

(c) Reconstructed edges E_2 from latent II.

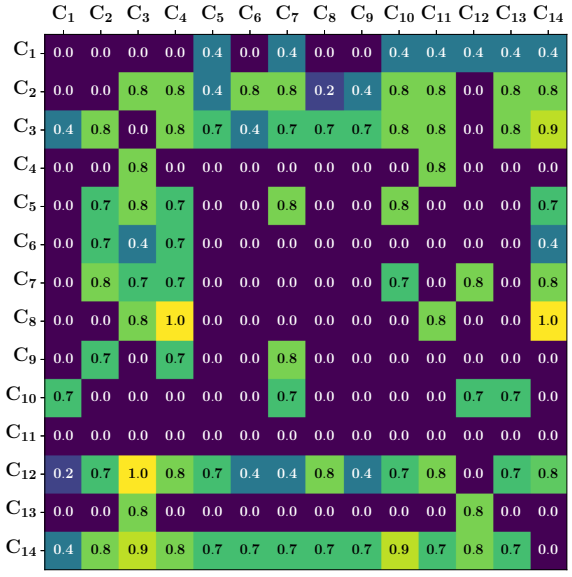

(d) Adjusted edge-reconstruction $\hat{E}_2$ from latent II.

Fig. 2: Autoencoding for the clinical depression FCM: (a) Edge matrix E corresponding to a 14-node FCM that models the causes of clinical depression. The nodes C_1–C_{14} from the 1st column of Table I are along the rows and columns. The source nodes are along the rows and the target nodes are along the columns. The element on the i^{th} row and j^{th} column gives the weight on the edge from C_i to C_j. Brighter color on the edge matrix corresponds to bigger edge weight or strength. (b) Reconstructed edge matrix E_1 from the encoded latent I summary. The reconstruction is more accurate because the input text was detailed even if it sounded unnatural. (c) Reconstructed edge matrix E_2 from the encoded latent II summary that refined the encoded text with the content editing prompt or sub-task. The reconstruction is not as accurate because the input text was not as detailed although it sounded natural. Many non-zero edge weights in E changed to zero in E_2. The edge weights that correspond to the flipped nodes C_4, C_9, and C_{10} from the 3rd column of Table I are negative. These negative edges are in red. (d) The adjusted reconstructed edge matrix from latent II text with flipped nodes. The reconstruction is lossy but it preserves the stronger causal connections with larger edge weights.

causal edges. The 1st column of Table I lists its nodes C_1–C_{14}. Figure 2a shows its edge matrix E. The edge matrix E uses brighter colors for causal edges with larger magnitudes.

The LLM agent completely encoded the FCM into a latent I summary consisting of 824 words. The LLM agent with the decoding prompt systematically reconstructed an FCM with 14 nodes but with 178 edges. The 2nd column of Table I lists the 14 nodes C_1–C_{14} and Figure 2b shows the edge matrix

TABLE I: Target and reconstructed nodes for the autoencoding of the clinical depression FCM

Concept Node	Target	Reconstruction from Latent I	Reconstruction from Latent II
$\mathbf{C_1}$	Psychomotor agitation	Psychomotor agitation	Psychomotor agitation
$\mathbf{C_2}$	Psychomotor retardation	Psychomotor retardation	Psychomotor retardation
$\mathbf{C_3}$	Depressive mood	Depressive mood	Depressive mood
$\mathbf{C_4}$	Reduced interest for daily function	Reduced interest for daily function	Interest for daily function
$\mathbf{C_5}$	Insomnia	Insomnia	Insomnia
$\mathbf{C_6}$	Hypersomnia	Hypersomnia	Hypersomnia
$\mathbf{C_7}$	Fatigue or loss of energy	Fatigue or loss of energy	Fatigue or loss of energy
$\mathbf{C_8}$	Recurrent thoughts of death	Recurrent thoughts of death	Thoughts of death
$\mathbf{C_9}$	Loss of appetite	Loss of appetite	Appetite
$\mathbf{C_{10}}$	Diminished ability to think or concentrate	Diminished ability to think or concentrate	Concentration
$\mathbf{C_{11}}$	Indecisiveness	Indecisiveness	Indecisiveness
$\mathbf{C_{12}}$	Feelings of worthlessness	Feelings of worthlessness	Worthlessness
$\mathbf{C_{13}}$	Extreme self-criticism	Extreme self-criticism	Self-criticism
$\mathbf{C_{14}}$	Depression	Depression	Depression

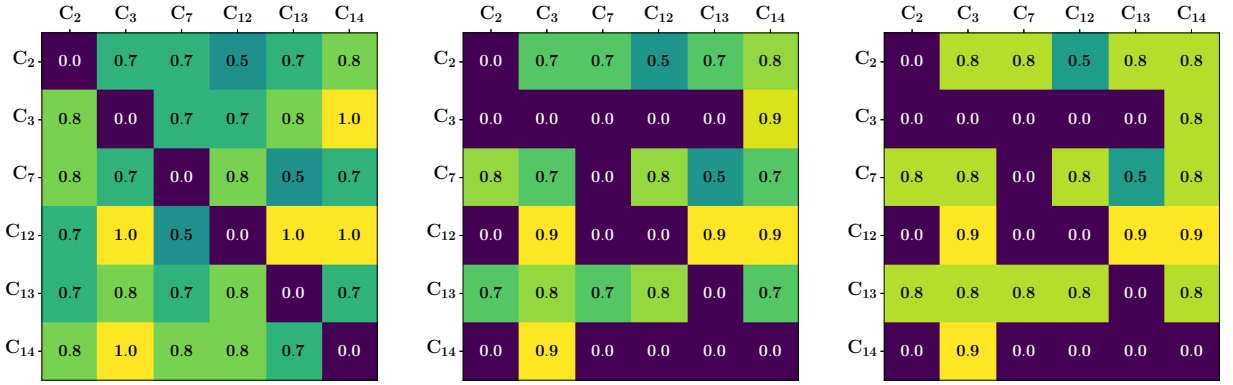

(a) Target edge matrix: E (b) Reconstructed edges from latent I: E_1 (c) Reconstructed edges from latent II: E_2

Fig. 3: FCM autoencoding for a strongly-connected depression FCM subset: (a) The edge matrix E corresponding to the subset of nodes C_2, C_3, C_7, C_{12}, C_{13}, and C_{14} from the depression FCM model described by Table I and Figure 2. The concept nodes from Table III index the rows and columns. The rows list the source nodes and the columns list the target nodes. The element on the i^{th} row and the j^{th} column gives the weight on the directed causal edge from the i^{th} source node to the j^{th} target node. The brighter colors correspond to the larger (stronger) causal edge weights. (b) Reconstructed edge matrix from the encoded latent I summary. Many non-zero edge weights in E are here zero but most of the bigger edge weights remain non-zero. (c) The reconstructed edge matrix from latent II summary that refined the encoded text with the content-editing prompt. Many non-zero edge weights in E changed to zero in $\hat{E}_2$ while most of the strongly connected edges remained non-zero.

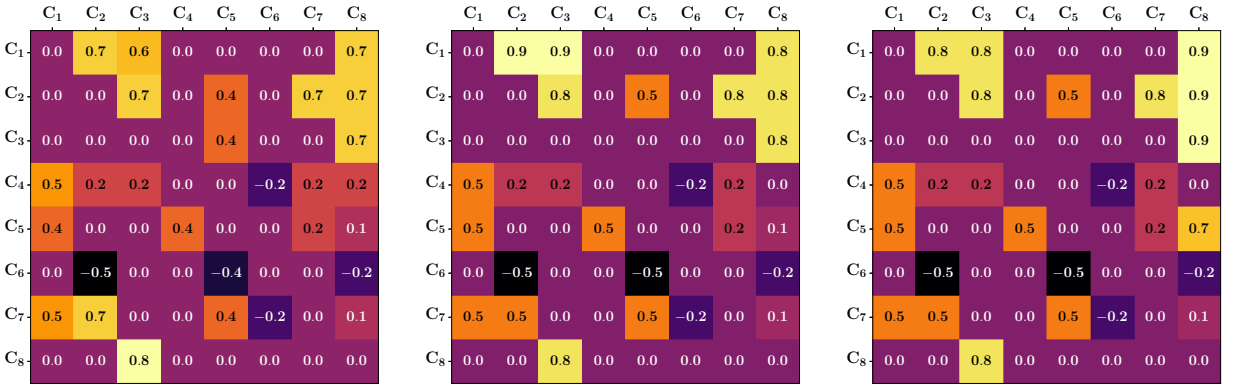

(a) Target edge matrix: E (b) Reconstructed edges from latent I: E_1 (c) Reconstructed edges from latent II: E_2

Fig. 4: FCM autoencoding for celiac disease classifier: (a) The edge matrix E corresponding to the 8-node FCM model that classifies celiac disease. The concept nodes from table IV index the rows and columns. The element on the i^{th} row and the j^{th} column gives the weight on the directed causal edge from C_i to C_j. The brighter colors correspond to larger (stronger) causal edge weights. (b) Reconstructed edge matrix from the encoded latent I summary. Many non-zero edge weights in E are zero but most of the high-magnitude edge weights remain non-zero. (c) Reconstructed edge matrix from the encoded latent II summary that refined the encoded text with the content editing prompt or sub-task. Many non-zero edge weights in E are here zero but most of the high-magnitude edge weights remain non-zero.

TABLE II: Reconstruction error with the autoencoding of the clinical depression FCM in Figure 2a

Metrics	Latent I	Latent II	Adjusted from Latent II
l_1-norm ↓	**14.56**	78.40	41.20
l_2-norm ↓	**1.588**	8.643	4.240
l_∞-norm ↓	**0.650**	2.002	0.653

E_1. The edge matrix E_1 is also colored such that the brighter color corresponds to the higher edge weight.

The LLM agent with the content editing prompt reworked the LLM agent's 824-word latent I text into 602 words of refined latent II text. The LLM agent with decoding prompts reconstructed a 14-node FCM from this latent II text, but this FCM only had 89 edges. Also 27 out of those 89 edges were negative because 3 out of the 14 nodes represented the opposite of the corresponding target node. The 2nd column of Table I lists the nodes C_1–C_{14} of this FCM and colors the "flipped" nodes in red. These nodes represent the opposite of their corresponding target node. Figure 2c shows the edge matrix E_2 where brighter colors correspond to higher edge-weight magnitudes or causal-degree magnitudes. It colors the negative edge weights in red.

The 2nd FCM samples 6 nodes C_2, C_3, C_7, C_{12}, C_{13}, and C_{14} from the first FCM. These nodes had the strongest causal connections among themselves. The 1st column of Table III lists the nodes of this FCM and Figure 3a gives its edge matrix E. The figure colors the edge matrix E so that brighter colors correspond to higher edge weights.

The LLM agent describes this FCM in 211 words. The LLM agent with decoding prompts then reconstruct a 6-node FCM with 20 edges from this raw text. The 2nd column of Table III lists the nodes of this FCM and Figure 3b shows the edge matrix from its latent I summary. The figure colors are such that the brighter colors correspond to larger edge weights.

The LLM agent with the content editing prompt reworked the LLM agent's latent I summary into 321 words of refined latent II summary. The LLM agent with the decoding prompts reconstructed a 6-node FCM with 20 edges from this refined text. The 3rd column of Table III and Figure 3c show the respective nodes and the reconstructed edge matrix from the latent II summary. The figure colors are such that brighter colors correspond larger edge magnitudes.

The 3rd FCM describes classification of celiac disease (CD) from tissue using 8 nodes and 28 edges [24]. The 1st column of Table IV and Figure 4a give the respective nodes and the edge matrix E of this FCM. The LLM agent with the encoding prompt described this FCM with 211 words of the latent I summary. LLM agent with decoding prompts then reconstructed a 6-node FCM with 26 edges. The 2nd column of Table IV gives its nodes and Figure 4b gives its edges. The figure colors are also such that the brighter color corresponds to a higher edge weight.

The LLM agent with the content editor prompt reworked the output of the first FCM into 295 words of refined latent II text. The LLM agent with the decoding prompt reconstructed a 8-node 26-edge FCM out of this text. The 3rd column of Table IV and Figure 4c give respective the nodes and the edge matrix E_2 of this FCM. The edge matrix shows the higher edge weights as brighter colors.

V. Discussion

Figures 2a and 2b show that the LLM agent with the encoding and the content editing prompt approximated an identity map from E to E_1 pretty well despite never comparing E_1 to E. This is due to the careful step-by-step systematic method used to map the FCM to text and to map the text back to an FCM. The carefully designed system instructions multi-prompted the LLM agent to follow this method exactly.

The latent I summary from the LLM agent with the encoding prompt sounded forced because the LLM focused more on accurately describing the FCM edges than sounding natural. The LLM agent with the content editing prompt reworded the latent I text summary to sound more natural but it came at the cost of reconstruction accuracy. Figures 2a and 2c show that the FCM reconstructed from the latent II summary of the LLM agent text missed a lot of edges. But even this lossy reconstruction preserved the stronger causal links of the FCM. The figures also show that edge weights on the 4th, 9th, and 10th rows and columns have flipped signs. The edge weight w_{49} flipped its sign twice and remained positive because it was in the 9th row and the 4th column. This occurred because the 4th, 9th, and 10th reconstructed nodes from the latent II summary represented the opposite of the corresponding causal variable from the target FCM. Table I's 1st and 3rd columns show this by highlighting the flipped nodes in red. The reconstructed FCM has "appetite" as the 9th node instead of "loss of appetite" in the target FCM.

Figure 2d flips the negative edges so we can compare it to 2a. The comparison shows that many non-zero edges from Figure 2a are zero in Figure 2d. But most of the high-weight edges remained non-zero. So even the lossy reconstruction preserves most of the important edges.

Table II measures the respective l_1, l_2, and l_∞ norms of the reconstruction errors in its rows 1–3. Its 1st and 2nd columns measure the respective error involved in reconstructing the edge matrix from the latent I and latent II summaries. The 3^{rd} column adjusts the reconstruction error from the latent II summary by flipping the edges connected to C_4, C_9, and C_{10}. The table shows that the latent I summary gave the best reconstructed edge matrix.

Figures 3a–3c and Figures 4a–4c show something similar. Some non-zero edge weights from the target FCM are zero in the both the reconstructed FCMs from the latent I and the latent II summaries. The two reconstructed FCMs differ little. Both the reconstructed FCMs preserve the stronger causal connections from the target FCM.

Tables I and IV show that there are some nodes in the FCM reconstructed from the latent II text that are slightly different from the corresponding target nodes. The tables highlight these nodes in blue. The 3rd column of Table IV calls the 7th node "mitotic activity" instead of "mitoses" as in the 1st column.

TABLE III: Strongly-connected subset of the clinical depression FCM

Concept Node	Target	Reconstructed from Latent I	Reconstructed from Latent II
$\mathbf{C_2}$	Psychomotor retardation	Psychomotor retardation	Psychomotor retardation
$\mathbf{C_3}$	Depressive mood	Depressive mood	Depressive mood
$\mathbf{C_7}$	Fatigue or loss of energy	Fatigue or loss of energy	Fatigue or loss of energy
$\mathbf{C_{12}}$	Feelings of worthlessness	Feelings of worthlessness	Feelings of worthlessness
$\mathbf{C_{13}}$	Extreme self-criticism	Extreme self-criticism	Extreme self-criticism
$\mathbf{C_{14}}$	Depression	Depression	Depression

TABLE IV: Concept nodes of the Celiac Disease (CD) classifier FCM

Concept Node	Target	Reconstructed from Latent I	Reconstructed from refined Latent II
$\mathbf{C_1}$	Villi blunting	Villi blunting	Villous blunting
$\mathbf{C_2}$	Crypt hyperplasia	Crypt hyperplasia	Crypt hyperplasia
$\mathbf{C_3}$	Intraepithelial lymphocyte infiltration	Intraepithelial lymphocyte infiltration	Intraepithelial lymphocyte infiltration
$\mathbf{C_4}$	Epithelial changes	Epithelial changes	Epithelial changes
$\mathbf{C_5}$	Lamina propria MNC infiltration	Lamina propria MNC infiltration	Lamina propria inflammation
$\mathbf{C_6}$	Decrescendo pattern	Decrescendo pattern	Decrescendo pattern
$\mathbf{C_7}$	Mitoses	Mitoses	Mitotic activity
$\mathbf{C_8}$	Class of celiac	Class of celiac	Classification of celiac

VI. Conclusion

A sequence of well-designed system instructions can multi-prompt an LLM agent to convert an FCM into text and then reconstruct the FCM back from the text by a new multi-step method. This approximates an identity map from the FCM to itself like an autoencoder but with human-interpretable text descriptions and does not compare the reconstructed output FCM with the input FCM. The LLM agent also explains its decisions unlike black-box neural autoencoder models.

References

[1] Bart Kosko. Fuzzy cognitive maps. *International journal of man-machine studies*, 24(1):65–75, 1986.

[2] Bart Kosko. Hidden patterns in combined and adaptive knowledge networks. *International Journal of Approximate Reasoning*, 2(4):377–393, 1988.

[3] Osonde A Osoba and Bart Kosko. Fuzzy cognitive maps of public support for insurgency and terrorism. *The Journal of Defense Modeling and Simulation*, 14(1):17–32, 2017.

[4] Guy Ziv, Elizabeth Watson, Dylan Young, David C Howard, Shaun T Larcom, and Andrew J Tanentzap. The potential impact of brexit on the energy, water and food nexus in the uk: A fuzzy cognitive mapping approach. *Applied Energy*, 210:487–498, 2018.

[5] Michael Glykas. *Fuzzy cognitive maps: Advances in theory, methodologies, tools and applications*, volume 247. Springer, 2010.

[6] Elpiniki I Papageorgiou. *Fuzzy cognitive maps for applied sciences and engineering: from fundamentals to extensions and learning algorithms*, volume 54. Springer Science & Business Media, 2013.

[7] Wojciech Stach, Lukasz Kurgan, and Witold Pedrycz. A divide and conquer method for learning large fuzzy cognitive maps. *Fuzzy Sets and Systems*, 161(19):2515–2532, 2010.

[8] Rod Taber, Ronald R Yager, and Cathy M Helgason. Quantization effects on the equilibrium behavior of combined fuzzy cognitive maps. *International Journal of Intelligent Systems*, 22(2):181–202, 2007.

[9] Antonis S Billis, Elpiniki I Papageorgiou, Christos A Frantzidis, Marianna S Tsatali, Anthoula C Tsolaki, and Panagiotis D Bamidis. A decision-support framework for promoting independent living and ageing well. *IEEE journal of biomedical and health informatics*, 19(1):199–209, 2014.

[10] Leland Gerson Neuberg. Causality: models, reasoning, and inference, by judea pearl, cambridge university press, 2000. *Econometric Theory*, 19(4):675–685, 2003.

[11] Shuhe Wang, Xiaofei Sun, Xiaoya Li, Rongbin Ouyang, Fei Wu, Tianwei Zhang, Jiwei Li, and Guoyin Wang. Gpt-ner: Named entity recognition via large language models. *arXiv preprint arXiv:2304.10428*, 2023.

[12] Google DeepMind. Gemini 2.5: Pushing the frontier with advanced reasoning and multimodality, 2025. Version 4.

[13] Diederik P Kingma and Max Welling. Auto-encoding variational bayes. *arXiv preprint arXiv:1312.6114*, 2013.

[14] Irina Higgins, Loic Matthey, Arka Pal, Christopher Burgess, Xavier Glorot, Matthew Botvinick, Shakir Mohamed, and Alexander Lerchner. β-vae: Learning basic visual concepts with a constrained variational framework. In *International conference on learning representations*, 2017.

[15] Christopher P Burgess, Irina Higgins, Arka Pal, Loic Matthey, Nick Watters, Guillaume Desjardins, and Alexander Lerchner. Understanding disentangling in β-vae. *arXiv preprint arXiv:1804.03599*, 2018.

[16] Bart Kosko and Olaoluwa Adigun. Bidirectional variational autoencoders. In *2024 International Joint Conference on Neural Networks (IJCNN)*, pages 1–9. IEEE, 2024.

[17] Pascal Vincent, Hugo Larochelle, Isabelle Lajoie, Yoshua Bengio, Pierre-Antoine Manzagol, and Léon Bottou. Stacked denoising autoencoders: Learning useful representations in a deep network with a local denoising criterion. *Journal of machine learning research*, 11(12), 2010.

[18] Yoshua Bengio, Li Yao, Guillaume Alain, and Pascal Vincent. Generalized denoising auto-encoders as generative models. *Advances in neural information processing systems*, 26, 2013.

[19] Mayu Sakurada and Takehisa Yairi. Anomaly detection using autoencoders with nonlinear dimensionality reduction. In *Proceedings of the MLSDA 2014 2nd workshop on machine learning for sensory data analysis*, pages 4–11, 2014.

[20] Lucas Theis, Wenzhe Shi, Andrew Cunningham, and Ferenc Huszár. Lossy image compression with compressive autoencoders. *arXiv preprint arXiv:1703.00395*, 2017.

[21] Anupriya Gogna and Angshul Majumdar. Discriminative autoencoder for feature extraction: Application to character recognition. *Neural Processing Letters*, 49(3):1723–1735, 2019.

[22] Qinxue Meng, Daniel Catchpoole, David Skillicom, and Paul J Kennedy. Relational autoencoder for feature extraction. In *2017 International joint conference on neural networks (IJCNN)*, pages 364–371. IEEE, 2017.

[23] Ashish Vaswani, Noam Shazeer, Niki Parmar, Jakob Uszkoreit, Llion Jones, Aidan N Gomez, Łukasz Kaiser, and Illia Polosukhin. Attention is all you need. *Advances in neural information processing systems*, 30, 2017.

[24] Abdollah Amirkhani, Elpiniki I Papageorgiou, Mohammad R Mosavi, and Karim Mohammadi. A novel medical decision support system based on fuzzy cognitive maps enhanced by intuitive and learning capabilities for modeling uncertainty. *Applied Mathematics and Computation*, 337:562–582, 2018.